Melt-processing and properties of coaxial fibers incorporating carbon nanotubes

Laforgue, Alexis; Champagne, Michel F.; Dumas, Jean; Robitaille, Lucie

Publisher's version / Version de l'éditeur:

Journal of Engineered Fibers and Fabrics, 7, 3, pp. 118-124, 2012-06-01

Melt-Processing and Properties of Coaxial Fibers Incorporating Carbon Nanotubes

ABSTRACT

Polypropylene-multiwalled carbon nanotubes (PP-CNT) composites were spun into fibers using melt-spinning methods. The CNT content was varied by diluting the commercial masterbatch with a low viscosity PP homopolymer grade. The conductivity as well as the mechanical properties of the fibers were systematically tested in order to find the optimal formulation. Post-stretching was used to improve the mechanical properties of the fibers as well as to decrease the fiber diameters. Fibers having a conductivity of 0.4 S/cm, a Young's modulus of 5.4 GPa and a tensile strength of 250 MPa were obtained after a three-fold stretching.

Trilayer coaxial fibers similar to data transfer coaxial cables (two conductive layers separated by an insulating layer) were then produced in a one-step melt-spinning method using a specially designed die, followed by solid state post-stretching.

INTRODUCTION

The textile industry is currently moving towards more and more sophisticated applications with the addition of specific high-end functionalities for various sectors, including health monitoring [1-3], sports [4], temperature regulation [5-6], electronics [7, 8], fashion [9, 10], etc. For the majority of these applications, data transmission and energy transfer within the fabric are major issues and require adequate conductive pathways. However, conducting materials, typically metals or carbon, are usually rigid, heavy and present limited flexibility.

Therefore, the development of new materials is required to produce conductive fibers that would match the mechanical properties of regular textile fibers and ensure a stable conductivity over time.

The incorporation of carbon nanotubes (CNTs) into polymer fibers has already been reported in the literature [11-15]. However, most studies focused on the mechanical properties (structural reinforcement) of the fibers, and the CNT content is typically too low in the composite to achieve a significant conductivity. The production of pure CNT fibers has also been reported in a number of publications. While these materials represent very good candidates for data/energy transmission into smart textiles, the production techniques are not mature enough to be scaled-up to an industrial level [16].

In this publication, we report the production of conductive PP-CNT fibers having high CNT contents for applications such as conductive pathways in smart textiles. Trilayer coaxial fibers having two conductive layers separated by an insulating layer (mimicking the conventional coaxial cables widely used for protected data transfer) were produced in one step using a melt-spinning process. The fibers were post-stretched in order to reduce their diameters and improve their mechanical properties. Their mechanical and electrical properties were thoroughly characterized before and after the post-stretching step.

MATERIALS AND METHODS

Materials

A commercial masterbatch of polypropylene (PP) filled with 20 wt% multiwalled carbon nanotubes (MWNT, Fibril MB3020-01) was supplied by Hyperion Catalysis (USA). The nature and properties of the masterbatch components are proprietary and were not disclosed by the supplier. Styrene-Ethylene-Butylene-Styrene elastomer (SEBS, Kraton G1652) was obtained from Kraton Polymers LLC (USA). Low viscosity PP homopolymer (Pro-Fax PF304, MI = 38, fiber grade) was obtained from Lyondell Basell USA.

Methods

Melt-dilution: PP-CNT masterbatch was diluted to desired CNT contents on a W&P twin-screw extruder using neat PP.

Monolayer fiber spinning: PP-CNTs fibers were processed using a twin-screw lab-scale extruder (DSM Xplore microcompounder) equipped with a single-hole die (diameter: 500 µm). The fibers were extruded at 210 °C and collected on a rotating godet with minimal stretching.

Multilayer fiber spinning: Multilayer fibers were produced using a Randcastle coextrusion line equipped with a specially designed single-hole die

allowing the extrusion of filaments having up to three coaxial layers made of three different materials (hole diameter: 1 mm). PP-CNT composites were extruded as the core and sheath layers, whereas SEBS was extruded as the intermediate layer. Melt temperatures for the PP-CNT and SEBS layers were set to 220 and 240 °C, respectively. The fibers were collected on a rotating godet with minimal stretching.

Post-processing: post-stretching of the fibers was carried out on a tensile testing machine (Instron 5582) equipped with an environmental chamber. Specially designed fiber holders were used in order to avoid clamping effects. The fibers were stretched up to 6 times their initial length, at a temperature slightly below the composite melting temperature (145 °C) and a speed of 50 mm/min.

Characterization: Strain-stress experiments were performed on an Instron 5548 microtester equipped with a special fiber holder. All experiments were carried out under controlled conditions (23 °C, 50 % relative humidity) at a speed of 5 mm/min. Scanning electron microscopy (SEM) was performed using a Hitachi S4700 microscope. A ca. 5 nm thick platinum layer was deposited on the fibers before imaging. The surface of the fibers was etched by successive soaking in a 7 g/L $KMnO_4$ solution in 6.5:3.5 H_2SO_4/H_3PO_4 for 1 h, 16 % H_2SO_4 for 2 min, 5 % H_2O_2 for 2 min and H_2O for 5 min, in order to degrade the amorphous parts of the polymer and let appear the MWNTs at the surface. Conductivity measurements were carried out on single fibers using an in-line four-point probe method and a VMP3 multipotentiostat (BioLogic Inc., France). Differential scanning calorimetry (DSC) measurements were made at 20°C/min using a model Q2000 from TA Instruments.

RESULTS & DISCUSSION

Monolayer fibers

The 20 wt% PP-CNT masterbatch was diluted to 5, 7.5, 10, 12.5 and 15 wt%. The resulting composites were then melt-spun using a lab-scale twin-screw extruder.

Composites with CNT contents higher than 12.5 wt% were difficult to melt-spin efficiently. Problems such as irregular fiber diameter and spin-line breaks were frequently observed. Large CNT aggregates coming from an incomplete dispersion process is most likely the source of the difficulties experienced at these high CNT contents. In contrast, melt- spinning composites with CNT contents lower than 12.5 wt% was regular and reproducible. The fibers extruded with composites at 12.5 wt% CNT and below have regular and smooth surfaces, as can be seen on Figure 1.

The conductivity of fibers incorporating different loadings of CNT was measured and results are presented in Figure 2. At a loading of 5 wt% CNT, the percolation threshold was already reached and a conductivity of 10^{-5} S/cm was measured (pure PP presents a conductivity around 10^{-10} S/cm).

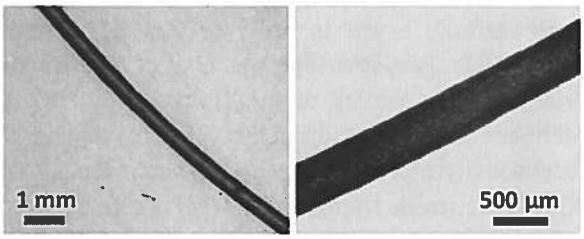

FIGURE 1. Microscopy images of a PP-CNT monolayer fiber at two different magnifications. CNT content: 12.5 wt%; Fiber diameter: 470 µm.

The conductivity increased significantly for a CNT loading of 7.5 wt%, then reached a relative plateau, demonstrating that a nearly complete percolation was reached. Conductivities larger than 0.5 S/cm were obtained for composites with CNT contents higher than 10 wt%, reaching 1 S/cm at CNT loadings above 12.5 wt%.

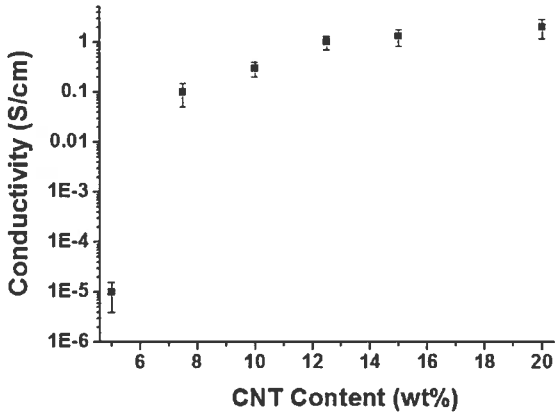

FIGURE 2. Conductivity of PP-CNT monolayer fibers for different CNT contents.

The mechanical properties of composite fibers containing between 5 and 12.5 wt% CNT were characterized. Figure 3 presents (a) typical stress-strain curves and (b) the Young's modulus and tensile

strength extracted from these data. The strain at break was around 11 % for all the fibers tested (Fig. 3a). However, both Young's modulus and tensile strength (maximum stress) were affected by the CNT content. As expected, the Young's modulus increased with CNT content, from an average value of 440 MPa at 5 wt% to 545 MPa at 12.5 wt%. The tensile strength followed the same trend and increased from 20 to 35 MPa when the CNT content was increased from 5 to 12.5 wt% (Fig. 3b).

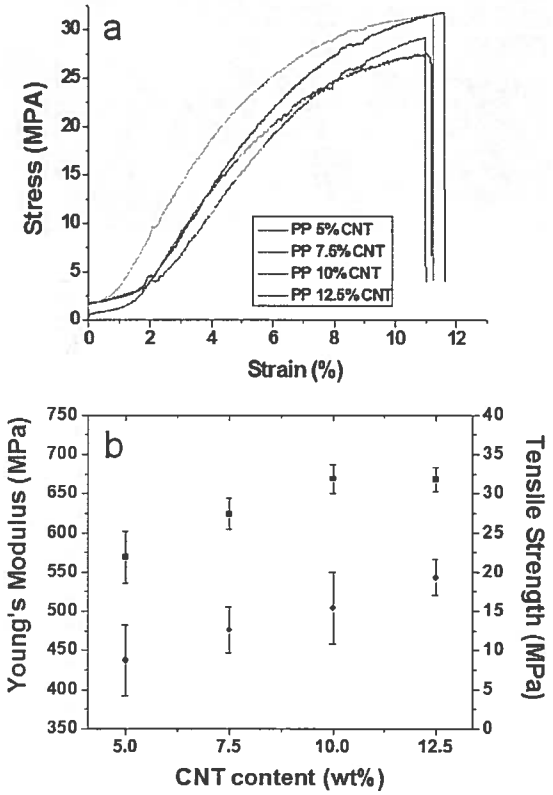

FIGURE 3. (a) Typical strain-stress curves of PP-CNT monolayer fibers for different CNT contents. (b) Corresponding Young's modulus (●) and tensile strength (■).

The best formulation, according to both mechanical and conductive properties, was the composite containing 12.5 wt% of CNT. The rest of the study was then carried out using this formulation.

In order to reduce the diameters and improve the mechanical properties of the fibers, they were post-stretched in the solid-state (just below the melting temperature of the composite). This procedure induced an alignment of the polymer chains, resulting in better interchain interactions and a significant increase in the polymer crystallinity [17-18].

The melting temperature of the composite was measured at 160°C from DSC measurements (Fig. 4). The temperature was then set at 145 °C for all post-stretching experiments.

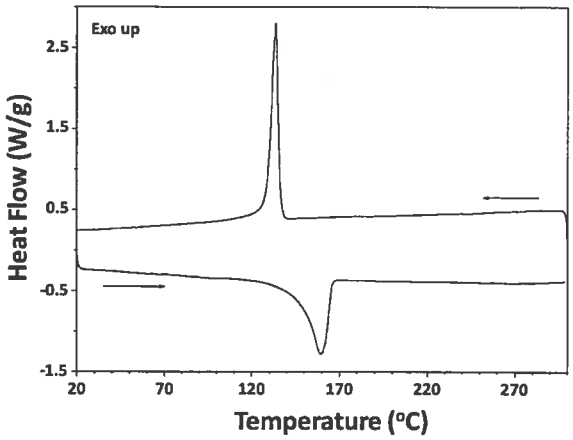

FIGURE 4. DSC curve for a PP-CNT composite containing 12.5 wt% CNT.

Figure 5 presents the mechanical properties of post-stretched fibers at different stretching ratios. The strain at break of the fibers was not significantly modified by the post-stretching process (Fig. 5a). However, their stiffness greatly increased in the process (Fig. 5b), with a Young's modulus reaching 6.8 GPa at $\lambda = 6$ (13-fold increase). It is interesting to note that the Young's modulus already increased by nearly one order of magnitude for a stretching ratio of 2. The tensile strength of the fibers also progressively improved with stretching, from 32 MPa before stretching to 415 MPa at $\lambda = 6$ (Fig. 5b).

The conductivity of the fibers was measured at each stretching ratio (Fig. 6) and a progressive loss of conductivity was observed with stretching.

This phenomenon has already been observed in the literature and was reported as an alignment of the nanotubes in the stretching direction, causing a progressive decrease of electrical percolation within the composite [12, 18-19]. Figure 7 shows that the MWNT bundles were progressively stretched and disentangled along the stretching direction. Even if individual nanotubes do not seem to be preferentially aligned in the stretching direction (most probably because of a very high degree of entanglement), the anisotropic disentanglement most likely causes a decrease of percolation between neighbouring bundles of MWNTs, the latter being progressively

separated by crystalline PP domains formed in the stretching process. This phenomenon results in a global decrease of the composite conductivity.

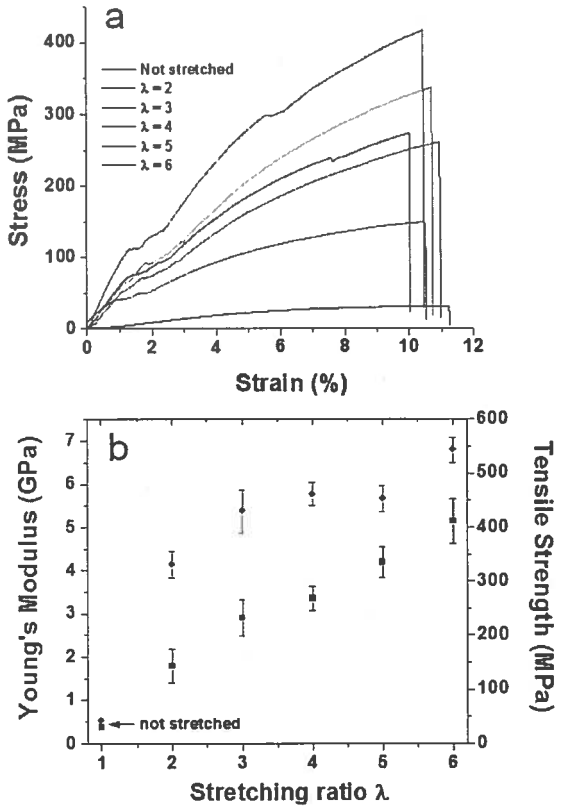

FIGURE 5. (a) Typical strain-stress curves of post-stretched PP-12.5% CNT monolayer fibers at different stretching ratios λ. (b) Corresponding Young's modulus (●) and tensile strength (■).

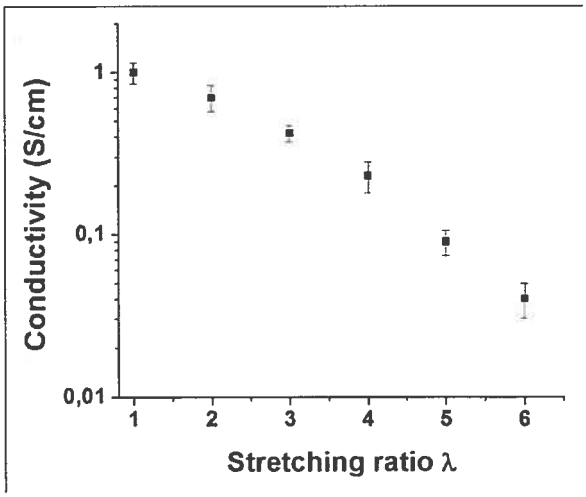

FIGURE 6. Conductivity of PP-12.5 % CNT fibers at different post-stretching ratios

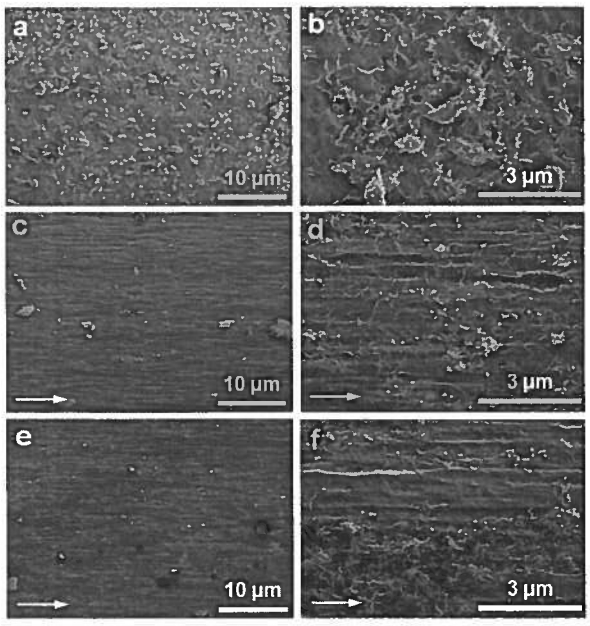

FIGURE 7. SEM images at different magnifications of a fiber surface before (a,b) and after stretching at a ratio of 3 (c,d) and 5 (e,f). The fibers were etched in strong oxidant solutions to remove the amorphous part of the PP and let the MWNTs appear at the surface. The arrows indicate the stretching direction.

Multilayer fibers

Fibers with two conductive layers separated by an insulating layer were produced using a coextrusion die adapted on a multilayer extrusion line. The resulting trilayer coaxial fibers had an average diameter of roughly 900 µm. Figures 8a and 8b show pictures of the as-extruded fibers. The coextruded fibers have rougher surfaces than the single layer fibers made on the lab-scale DSM extruder (Fig. 1 compared to Figure 8).

These surface features are most likely induced by flow instabilities generated during the extrusion of the viscous PP-CNT composites (peak pressure at 3500 psi was monitored at die entrance during processing). Surface roughness was minimized by reducing the extruder screw rotation speeds but could unfortunately not be totally eliminated.

The coaxiality of the fibers was verified by optical microscopy (Fig. 8c). The relative thickness of each layer could be controlled by varying the screw rotation speed of each extruder. Figure 7c shows cross-sections of fibers where the thickness of the core layer was kept constant while the intermediate and sheath layers' thicknesses were varied.

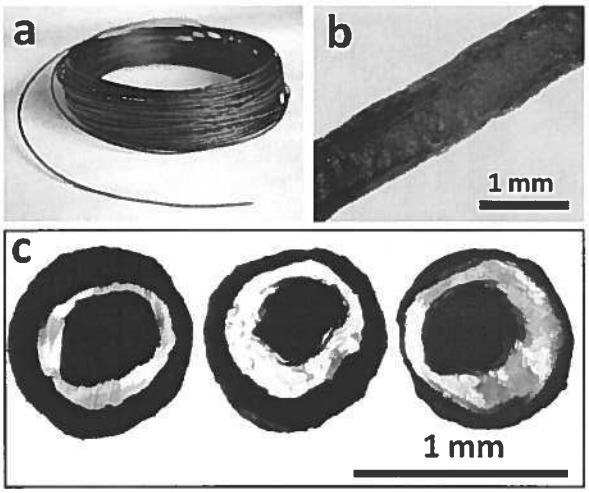

FIGURE 8. (a) and (b), images of trilayer fibers at different magnifications, (c) cross-section of fibers with varying relative thicknesses of the two external layers (from left to right : increasing intermediate layer and decreasing sheath layer). Fibers average diameter: 900 μm

The fibers were then post-stretched at 145 °C at a speed of 50 mm/min up to $\lambda = 4$, decreasing their diameter from approximately 900 μm to 250-300 μm (Fig. 9). The coaxiality of the trilayer fibers was preserved during the post-stretching process..

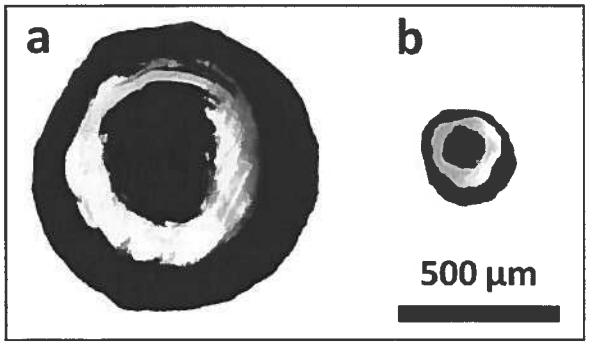

FIGURE 9. Cross-sections of a trilayer fiber (a) before stretching (diameter 900 μm) and (b) after stretching ($\lambda = 4$, diameter 280 μm).

The mechanical properties of the trilayer fibers are presented in Figure 10. The strain at break of the trilayer fibers was typically lower than that of the monolayer fibers: 6-8% compared to around 11 % for the monolayer fibers (Figs. 3 and 5). Given that the intermediate layer of the trilayer structure is an elastomer with much higher maximum elongation than the PP-CNT composites, the reduced strain at break shows that the interfaces between the layers act as structural defects in the fibers. Indeed, the stress-strain curve of the unstretched fiber (Fig. 10a) showed three successive fractures, corresponding to the failure of each layer. These independent fractures suggest that the layers are not strongly bound to each other.

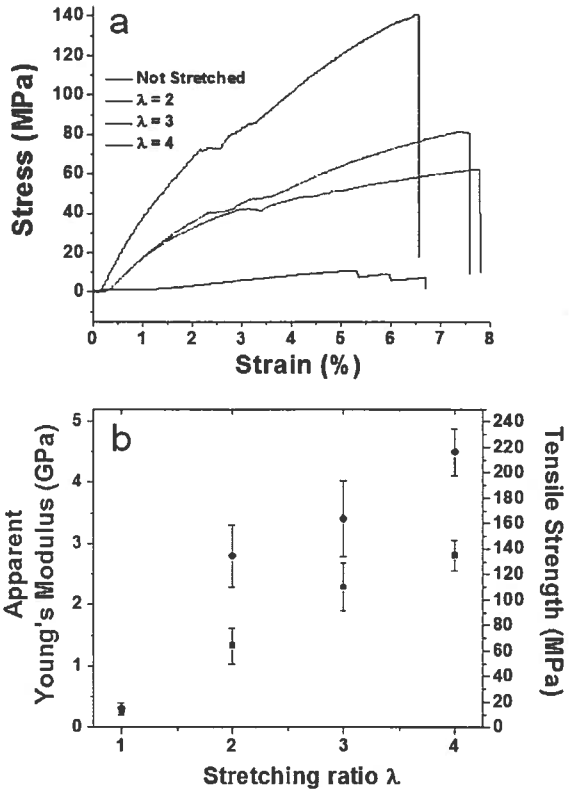

FIGURE 10. (a) Typical strain-stress curves of trilayer fibers at different stretching ratios λ. (b) Corresponding apparent Young's modulus (●) and tensile strength (■).

After stretching however, these phenomena are much less obvious, indicating that the layers are more tightly bound to each other. The strain at break was not improved after post-stretching, but the fibers strength significantly increased. Although the Young's modulus of the fiber refers to a system of materials rather than an individual material (we hence named it "apparent Young's modulus"), its value is useful to estimate the fiber's stiffness. As observed for the monolayer fibers, post-stretching generated a 10-fold increase in the modulus of fibers stretched at $\lambda = 2$ (0.3 to 2.8 GPa) and a 15-fold increase for those processed at $\lambda = 4$ (0.3 to 4.5 GPa). The tensile strength was also improved, from 12.5 MPa before stretching to 65 and 135 MPa at $\lambda = 2$ and 4, respectively (cf. Fig. 10b).

Even after post-stretching, these values were lower than the PP-CNT monolayer fibers, most probably due to addition of an elastomeric intermediate layer. However, these post-stretched fibers are sufficiently strong to be sewn or weaved into regular textiles.

CONCLUSIONS AND PERSPECTIVES

PP-CNT composite fibers with significant electrical conductivities were produced by melt-spinning of high CNT content composites. The mechanical properties of the fibers were greatly improved by a subsequent solid-state stretching process. The latter step also led to a decrease in conductivity due to an alignment of the CNT in the drawing direction.

Trilayer coaxial fibers similar to data transfer coaxial cables were also produced using a one-step melt-spinning method, followed by solid state post-stretching. The coaxiality of the layers was maintained during the post-stretching step. The resulting coaxial fibers had diameters around 300 µm, average Young's modulus of 4.5 GPa and tensile strength of 135 MPa.

To further improve the electrical properties of the fibers, an additional post-annealing treatment of the fibers under constant stress will be investigated. This should allow the aligned CNT to relax into a more isotropic state, hence improving the electrical conductivity within the composite [20]. Data and energy transfer in the core of the fibers will also be part of future investigations.

ACKNOWLEDGEMENTS

The authors acknowledge Robert Lemieux, François Vachon, Nicole Côté, Manon Plourde, Jacques Dufour and Karine Théberge from NRC-IMI, for their respective technical participation to the experiments.

REFERENCES

[1] Carpi, F.; De Rossi, D.; Electroactive Polymer-Based Devices for e-Textiles in Biomedicine. *IEEE Transactions on Information Technology in Biomedicine*, 2005, 9(3), 295-318.

[2] Catrysse, M.; Puers, R.; Hertleer, C.; Langenhove, L.V.; Egmond, H.V.; Matthys, D.; Towards the integration of textile sensors in a wireless monitoring suit; *Sensors and Actuators* A, 2004, 114, 302-311.

[3] Loriga, G.; Taccini, N.; Pacelli, M.; Paradiso, R.; Flat Knitted Sensors for Respiration Monitoring; *IEEE Industrial Electronics Magazine*, 2007, 1(3), 5-8.

[4] Textronics, Inc. (USA) website : http://www.textronicsinc.com/

[5] Gorix, Ltd. (UK) website : http://www.gorix.com/

[6] Outlast Technologies, Inc. (USA) website : http://www.outlast.com/

[7] Jung, S.; Lauterbach, C.; Strasser, M. and Weber, W.; Enabling Technologies for Disappearing Electronics in Smart Textiles; *IEEE International Solid-State Circuits Conference*, 2003, 386-387.

[8] Hamedi, M.; Forchheimer, R. and Inganäs, O.; Towards woven logic from organic electronic fibres; *Nature Materials*, 2007, 6, 357-362.

[9] Berzowska, J.; Electronic Textiles: Wearable Computers, Reactive Fashion, and Soft Computation; *Textile*, 2005, 3(1), 2-19.

[10] Buechley, L.; A Construction Kit for Electronic Textiles. *IEEE International Symposium on Wearable Computers*, 2006, 83-90.

[11] Spitalsky, Z.; Tasis, D. ; Papagelis, K. And Galiotis, G.; Carbon nanotube-polymer composites: Chemistry, processing, mechanical and electrical properties; *Progress in Polymer Science*, 2010, 35, 357-401.

[12] Haggenmueller, R.; Gommans, R. R.; Rinzler, A. G.; Fischer J. E.; Winey, K. I.; Aligned single-wall carbon nanotubes in composites by melt processing methods; *Chemical Physics Letters*, 2000, 330, 219-225.

[13] Kearns, J. C. And Shambaugh, R. L.; Polypropylene Fibers Reinforced with Carbon Nanotubes; *Journal of Applied Polymer Science*, 2002, 86, 2079-2084.

[14] McIntosh, D. ; Khabashesku, V. N. and Barrera, E. V.; Benzoyl Peroxide Initiated In Situ Functionalization, Processing, and Mechanical Properties of Single-Walled Carbon Nanotube-Polypropylene Composite Fibers; *The Journal of Physical Chemistry C.*, 2007, 111, 1592-1600.

[15] Perrot, C.; Piccione, P. M.; Zakri, C.; Gaillard, P.; Poulin, P.; Influence of the Spinning Conditions on the Structure and Properties of Polyamide 12/Carbon Nanotube Composite Fibers; *Journal of Applied Polymer Science*, 2009, 114, 3515-3523.

[16] Behabtu, N.; Greena, M. J; Pasquali, M.; Carbon nanotube-based neat fibers; *Nano Today*, 3(5-6), 24-34.

[17] Hu, X.; Alcock, B.; Loos, J.; The influence of drawing temperature on mechanical properties and organization of melt spun polyethylene solid-state drawn in the pseudo-affine regime; *Polymer*, 2006, 47, 2156-2162.

[18] Deng, H.; Zhang, R.; Bilotti, E.; Loos, J.; T. Peijs, T.; Conductive Polymer Tape Containing Highly Oriented Carbon Nanofillers; *Journal of Applied Polymer Science*, 2009, 113, 742-751.

[19] Pötschke, P.; Bruünig, H.; Janke, A.; Fischer, D.; Jehnichen, D.; Orientation of multiwalled carbon nanotubes in composites with polycarbonate by melt spinning; *Polymer*, 2005, 46, 10355–10363.

[20] Deng, H.; Skipa, T.; Bilotti, E.; Zhang, R.; Lellinger, D.; Mezzo, L.; Fu, Q.; Alig, I.; Peijs, T.; *Advanced Functional Materials*, 2010, 20, 1424-1432.